The Astrophysical Journal Letters, 763:L13 (6pp), 2013 January 20 doi:10.1088/2041-8205/763/1/L13

RADIO DETECTION OF THE *FERMI*-LAT BLIND SEARCH MILLISECOND PULSAR J1311−3430

P. S. Ray[1], S. M. Ransom[2], C. C. Cheung[3,19], M. Giroletti[4], I. Cognard[5,6], F. Camilo[7,8], B. Bhattacharyya[9], J. Roy[10], R. W. Romani[11], E. C. Ferrara[12], L. Guillemot[13], S. Johnston[14], M. Keith[14], M. Kerr[11], M. Kramer[13,15], H. J. Pletsch[16,17], P. M. Saz Parkinson[18], and K. S. Wood[1]

[1] Space Science Division, Naval Research Laboratory, Washington, DC 20375-5352, USA; Paul.Ray@nrl.navy.mil
[2] National Radio Astronomy Observatory (NRAO), Charlottesville, VA 22903, USA
[3] National Academy of Sciences, Washington, DC 20001, USA
[4] INAF Istituto di Radioastronomia, I-40129 Bologna, Italy
[5] Laboratoire de Physique et Chimie de l'Environnement, LPCE UMR 6115 CNRS, F-45071 Orléans Cedex 02, France
[6] Station de radioastronomie de Nançay, Observatoire de Paris, CNRS/INSU, F-18330 Nançay, France
[7] Columbia Astrophysics Laboratory, Columbia University, New York, NY 10027, USA
[8] Arecibo Observatory, HC3 Box 53995, Arecibo, PR 00612, USA
[9] Inter-University Centre for Astronomy and Astrophysics, Pune 411 007, India
[10] National Centre for Radio Astrophysics, Tata Institute of Fundamental Research, Pune 411 007, India
[11] W. W. Hansen Experimental Physics Laboratory, Kavli Institute for Particle Astrophysics and Cosmology, Department of Physics and SLAC National Accelerator Laboratory, Stanford University, Stanford, CA 94305, USA
[12] NASA Goddard Space Flight Center, Greenbelt, MD 20771, USA
[13] Max-Planck-Institut für Radioastronomie, Auf dem Hügel 69, D-53121 Bonn, Germany
[14] CSIRO Astronomy and Space Science, Australia Telescope National Facility, Epping NSW 1710, Australia
[15] Jodrell Bank Centre for Astrophysics, School of Physics and Astronomy, The University of Manchester, Manchester M13 9PL, UK
[16] Max-Planck-Institut für Gravitationsphysik, Albert-Einstein-Institut, D-30167 Hannover, Germany
[17] Leibniz Universität Hannover, D-30167 Hannover, Germany
[18] Santa Cruz Institute for Particle Physics, Department of Physics and Department of Astronomy and Astrophysics, University of California at Santa Cruz, Santa Cruz, CA 95064, USA
Received 2012 October 23; accepted 2012 December 5; published 2013 January 2

ABSTRACT

We report the detection of radio emission from PSR J1311−3430, the first millisecond pulsar (MSP) discovered in a blind search of *Fermi* Large Area Telescope (LAT) gamma-ray data. We detected radio pulsations at 2 GHz, visible for <10% of ∼4.5 hr of observations using the Green Bank Telescope (GBT). Observations at 5 GHz with the GBT and at several lower frequencies with Parkes, Nançay, and the Giant Metrewave Radio Telescope resulted in non-detections. We also report the faint detection of a steep spectrum continuum radio source (0.1 mJy at 5 GHz) in interferometric imaging observations with the Jansky Very Large Array. These detections demonstrate that PSR J1311−3430 is not radio quiet and provide additional evidence that radio-quiet MSPs are rare. The radio dispersion measure of 37.8 pc cm^{-3} provides a distance estimate of 1.4 kpc for the system, yielding a gamma-ray efficiency of 30%, typical of LAT-detected MSPs. We see apparent excess delay in the radio pulses as the pulsar appears from eclipse and we speculate on possible mechanisms for the non-detections of the pulse at other orbital phases and observing frequencies.

Key word: pulsars: individual (PSR J1311−3430)

Online-only material: color figures

1. INTRODUCTION

The Large Area Telescope (LAT) on the *Fermi Gamma-ray Space Telescope* has been surveying the gamma-ray sky in the 20 MeV to 300 GeV band since 2008 August. The LAT survey has vastly increased the population of known gamma-ray emitting sources including pulsars, blazars, supernova remnants, pulsar wind nebulae, and more. However, in the second LAT source catalog (hereafter 2FGL; Nolan et al. 2012), 575 (31%) of the 1873 sources were not associated with any known counterpart. The properties of the unassociated source population have been studied (Ackermann et al. 2012) and they roughly fall into two categories of "pulsar-like" (non-variable with spectra that exhibit significant curvature) and "blazar-like" (highly variable, spectra without strong cutoffs).

Beyond studying their gamma-ray emission properties, the most promising way to make progress on understanding and identifying the unassociated sources is through multi-wavelength observations. As a striking example, deep searches for radio pulsars in the pulsar-like population have led to the discovery of 43 new millisecond pulsars (MSPs) and four young and middle-aged pulsars (Ray et al. 2012). Of course, since all of these pulsars were discovered in radio searches, these discoveries do not probe the possible radio-quiet MSP population, which must be discovered in other wavelengths.

The first strong candidate radio-quiet MSP was found through X-ray and optical studies of the bright unassociated source 2FGL J2339.6−0532 (Romani & Shaw 2011; Kong et al. 2012). The orbital modulation of the optical emission suggests that the system comprises a "black widow"-type MSP (King et al. 2005) in a 4.6 hr orbit around a low-mass companion. Very recently, radio pulsations from this source were reported (Ray 2012), confirming that it is indeed an MSP whose wind is evaporating its companion.

More recently, Romani (2012) identified another such system associated with 2FGL J1311.7−3429 (hereafter J1311; see also Kataoka et al. 2012). In this case, the optical modulation

[19] National Research Council Research Associate; resident at Naval Research Laboratory, Washington, DC 20375, USA.

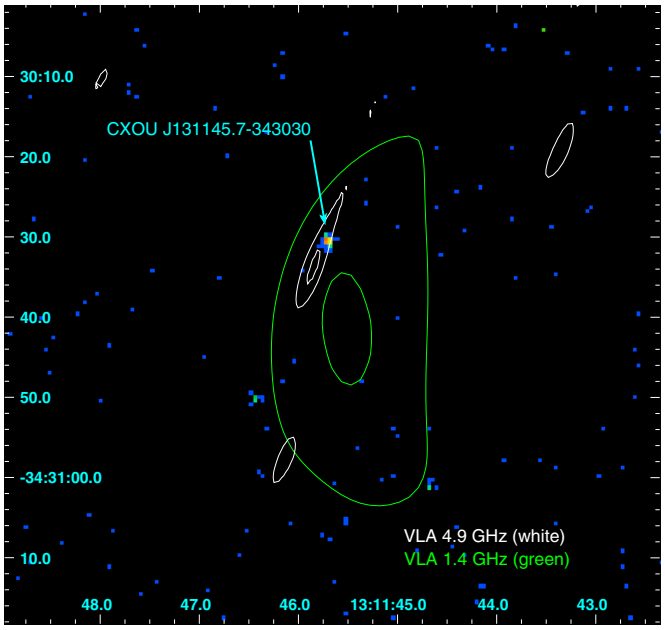

Figure 1. VLA radio contours at 5 GHz (white; 80 and 113 μJy beam^{-1}) and 1.4 GHz (green; 250 and 354 μJy beam^{-1}) overlaid onto a *Chandra* 0.5–7 keV image of the region showing the X-ray point source, CXOU J131145.7−343030 from Cheung et al. (2012), found coincident with the pulsar. The synthesized beams are $16\farcs2 \times 3\farcs5$ (position angle, P.A. $= -26\fdg1$) and $49\farcs1 \times 14\farcs7$ (P.A. $= -22\fdg9$), respectively.

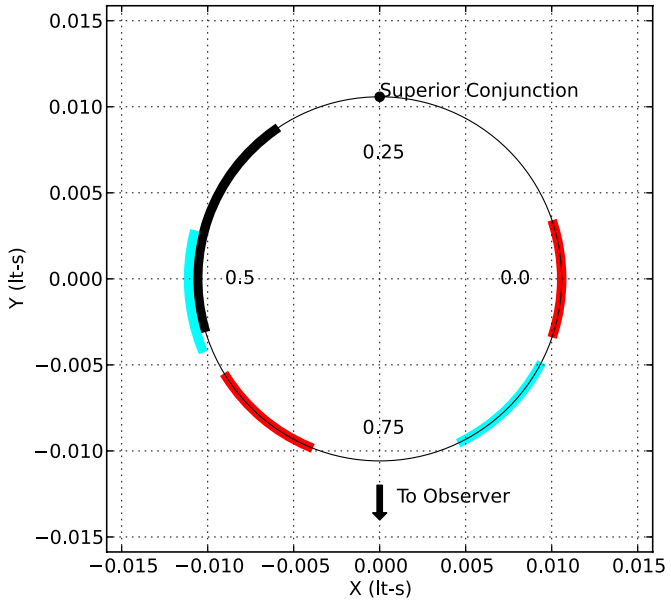

Figure 2. Figure showing the orbit of the pulsar with the phase range of the 2 GHz radio pulsation detection marked in gray. The VLA observation intervals centered at phases 0.51 and 0.87 (5 GHz; cyan) and 0.64 and 1.00 (1.4 GHz; red) are marked. Orbital phase is measured as a fraction of the orbit from the ascending node (when the pulsar crosses the plane of the sky heading away); orbital phases of 0.0, 0.25, 0.5, and 0.75 are noted. Superior conjunction (e.g., mid-eclipse time) is also shown.

revealed an orbital period of 1.56 hr, the shortest of any known MSP, with a companion that is very hydrogen poor. Using the optical source position and information about the orbital parameters from the optical measurements, Pletsch et al. (2012) discovered the first gamma-ray MSP found in a blind search, PSR J1311−3430, with period $P = 2.56$ ms. This discovery confirmed the black widow pulsar nature of the system and yielded important parameters such as the spin-down luminosity ($\dot{E} = 4.9 \times 10^{34}$ erg s^{-1}) of the pulsar and the precise orbital parameters, including the projected semimajor axis of the orbit (10.6 lt-ms). As the pulsar was discovered in the gamma-ray band, it was a candidate for being the first radio-quiet MSP. Analysis of archival 820 MHz and 350 MHz radio observations with the Robert C. Byrd Green Bank Telescope (GBT) resulted in no detections (Pletsch et al. 2012). However, as Romani (2012) pointed out, the low-frequency radio emission could be scattered or absorbed and thus be undetectable from Earth, even if the pulsar radio beam was directed at Earth. Because scattering and absorption of the radio emission are strong functions of frequency, this motivates further radio observations at higher frequencies.

In this Letter, we report the detection of radio emission from PSR J1311−3430, both in continuum imaging observations with the Karl G. Jansky Very Large Array (VLA) and in a radio pulsation search with the GBT at 2 GHz. This confirms that PSR J1311−3430 is indeed a radio MSP with the beam sweeping across Earth, completing the chain from unassociated gamma-ray source to optical identification to gamma-ray pulsation detection to radio detection.

2. OBSERVATIONS AND RESULTS

2.1. VLA Imaging Observations

We observed the J1311 field on 2011 January 14 with the VLA (Perley et al. 2011) while in the C-array (program S2270). Observations were made at 1.4 and 5 GHz using two 128 MHz wide intermediate frequencies centered at 1.327 + 1.455 GHz and 4.895 + 5.023 GHz, respectively. In the 1 hr observing run, we obtained two 9 minute target scans per frequency bracketed with scans of a phase calibrator (J1316−3338), while the primary flux calibrator was 3C 286.

An analysis of the 5 GHz data revealed an unresolved (ratio of the peak to integrated flux density ∼1; Condon 1997) 0.10 ± 0.04 mJy point source at a position (J2000.0), R.A. $= 13^{\rm h}11^{\rm m}45\fs78$ ($\pm 1\farcs0$) and decl. $= -34\arcdeg30\arcmin31\farcs2$ ($\pm 1\farcs7$), consistent with the pulsar (i.e., the pulsar is within the VLA synthesized beam). In the 1.4 GHz image, there is a 0.99 ± 0.44 mJy source (peak $= 0.33 \pm 0.11$ mJy beam^{-1}) that shows evidence of extension, with a centroid that is slightly offset (∼13″) from the 5 GHz position (Figure 1). Imaging the two scans of J1311 at each frequency separately (see Figure 2 for the corresponding orbital phases) did not reveal any statistically significant flux changes.

2.2. Radio Pulsar Observations

After the discovery of the gamma-ray pulsations by Pletsch et al. (2012), we performed a series of radio observations to search for radio pulsations from the pulsar. Given the non-detections at 820 and 350 MHz (Ransom et al. 2011; Pletsch et al. 2012), and the 1.4 and 5 GHz VLA detections (Section 2.1), the priority was on higher frequency observations to minimize the effects of scattering, dispersion, and absorption. For completeness, we include the earlier GBT observations in our analysis. The observations performed are listed in Table 1. All observations are made with two summed polarizations. In all cases, we compute the pulsed flux density limits using the modified radiometer equation as described by Ray et al. (2011). We assume a pulse duty cycle of 0.1 and a signal-to-noise threshold for detection of 5σ.

Table 1
Radio Pulsar Observations

Obs. Code	Date	t_{obs} (s)	Orb. Phase	T_{sys}[a] (K)	S_{min}[b] (μJy)
GBT-820	2011 Jan 15	2577	0.092–0.550	38	53 (22)
GBT-820	2011 Dec 10	1723	0.346–0.652	38	53 (22)
GBT-820	2012 Aug 24	900	0.295–0.455	38	53 (22)
GBT-820	2012 Aug 25	900	0.977–0.137	38	53 (22)
GBT-350	2012 Feb 24	1287	0.339–0.568	104	203 (22)
GBT-S	2012 Jul 28	4939	0.859–0.737	26	**114 ± 60**
GBT-S	2012 Aug 19	11697	2 orbits	26	20 (36)
GBT-S	2012 Aug 25	900	0.346–0.506	26	20 (36)
GBT-C	2012 Jul 28	4552	0.931–0.740	22	16 (115)
GMRT-607	2011 Feb 15	3386	0.108–0.710	108	445 (117)
GMRT-607	2011 Jun 23	7246	0.349–0.637	108	445 (117)
GMRT-322	2012 Aug 15	3607	0.844–0.485	137	184 (18)
Parkes-AFB	2012 Mar 22	3600	0.606–0.246	29	115 (114)
Parkes-AFB	2012 Jul 11	3600	0.337–0.977	29	115 (114)
Parkes-AFB	2012 Jul 12	3600	0.025–0.665	29	115 (114)
Parkes-AFB	2012 Jul 16	3600	0.092–0.732	29	115 (114)
Parkes-AFB	2012 Aug 17	1635	0.403–0.694	29	115 (114)
Parkes-AFB	2012 Aug 17	5357	0.766–0.718	29	115 (114)
Parkes-AFB	2012 Aug 24	4500	0.130–0.930	29	115 (114)
NRT-L	2012 Jul 16	2512	0.182–0.628	39	48 (54)
NRT-L	2012 Jul 21	2997	0.563–0.096	39	48 (54)
NRT-L	2012 Aug 23	736	0.368–0.499	39	48 (54)
NRT-L	2012 Sep 1	2996	0.788–0.320	39	48 (54)
NRT-L	2012 Sep 24	1257	0.094–0.317	39	48 (54)

Notes.
[a] System temperature including receiver temperature (T_{rec}) and sky temperature (T_{sky}) from scaling the 408 MHz Haslam map to the observing frequency and adding 2.7 K for the cold sky background.
[b] Flux density limits are computed for a standard integration time of 1000 s at the observing frequency (corresponding to the duration where pulses were seen in the one detection), with the equivalent limit at 1400 MHz in parentheses, assuming a spectral index of −1.8. The bold value is the detected flux density in this observation, scaled to 1.4 GHz.

2.2.1. Green Bank Telescope

We observed the J1311 field with the GBT (project GBT/12A-487) with the GUPPI backend (DuPlain et al. 2008) on 2012 July 28 for 1.4 hr at 2 GHz and 1.3 hr at 5 GHz with a bandwidth of 800 MHz and 40.96 μs sampling. At 2 GHz we used 2048 frequency channels, while at 5 GHz we used 1024 channels. We obtained a second GBT observation on 2012 August 19 spanning 3 hr at 2 GHz, with the same observing setup. At the start of each observation, we observed the pulsar B1257+12, which was detected each time.

We analyzed the data using PRESTO (Ransom 2001) to first excise strong radio frequency interference (RFI) signals and then fold the data using an ephemeris based on the parameters of the gamma-ray pulsation discovery. The RFI environment during these observations was rather benign, requiring blanking of some narrowband signals amounting to <7% of the data. The only free parameter in the search was dispersion measure (DM). In our first 2 GHz observation, we detected radio pulsations during a ∼1100 s interval beginning at MJD (UTC) 56136.908 with a DM of 37.84 ± 0.26 pc cm^{-3} (see Figure 3). The significance of the detection over the 1100 s where the pulse is visible, after correcting for the 6400 trials in the DM search, is 10.3 σ. This significance is computed from the profile using the χ^2 test for excess variance. It differs from the value shown in Figure 3 because it is based on a subset of the data that exclude the first 600 s where no signal is apparent. Based on the detection significance and the sensitivity of our observations, we estimate a mean flux density of 60 ± 30 μJy. No pulsations were seen in the 5 GHz observation or the second 2 GHz observation.

As seen in Figure 3, the signal significance peaks at a frequency slightly offset ($\Delta\nu \sim 5\times10^{-3}$ Hz) from that predicted by the gamma-ray ephemeris. The orbital phase at the start of the interval in Figure 3 is 0.24, when the pulsar is expected to be at mid-eclipse, so this is apparently caused by excess delay in the radio pulse as the pulsar is emerging from eclipse, as is seen in many eclipsing MSPs. To test this, we folded only the data starting after 600 s and the detection significance peaks at the predicted period and period derivative. In addition, we generated 15 times of arrival (TOAs) across the observation, with 114 s of integration per TOA. We discarded the first three with no apparent pulsed detection. Looking at only the last 10 TOAs, the measured period is consistent with that predicted from the gamma-ray ephemeris. The two earlier TOAs appear to show a changing delay that is about 0.6 ms (1/4 of a pulse period) just as the pulse becomes visible.

2.2.2. Parkes

We made a total of seven observations at 1.4 GHz using the Parkes telescope with the Analog Filter Bank (AFB) backend recording 256 MHz of bandwidth (0.5 MHz channels sampled every 125 μs) and analyzed them in the same manner as described above. No pulsations were detected in any of the observations.

2.2.3. Nançay

We performed five observations with the Nançay Decimetric Radio Telescope (NRT) around 1.5 GHz ranging from 700 to 3000 s. We used a 512 MHz bandwidth divided into 1024 channels with 64 μs sampling. Dedispersion at a DM of 37.84 pc cm^{-3} and folding using the known parameters did not produce any detectable pulsations. The offsets from the gamma-ray pulsation position are negligible when compared to the beam size of the telescope.

2.2.4. Giant Metrewave Radio Telescope

We analyzed two archival 607 MHz (32 MHz bandwidth) observations made using the Giant Metrewave Radio Telescope (GMRT) incoherent array in early 2011 as part of a pulsar search of LAT unassociated sources. Folding these data with the timing model from the LAT discovery resulted in no detections. Later with the precise pulsar position, we made sensitive coherent array observations at 322 MHz, also with 32 MHz bandwidth (Roy et al. 2010). Again, no pulsations were detected.

2.3. Radio/Gamma-ray Profiles

We computed phase-aligned radio and gamma-ray profiles, shown in Figure 4. The gamma-ray profiles are computed from the same weighted LAT events as in Pletsch et al. (2012) spanning 2008 August 4 to 2012 July 10. The phase was computed according to the pulsar ephemeris of Pletsch et al. (2012), with the fiducial phase shifted to correctly align with the radio profile, using a DM of 37.84 pc cm^{-3}. The radio profile at 2 GHz was constructed from the GBT observation at 2 GHz using the 1100 s of data where the pulsar signal is apparent.

Both the radio and gamma-ray profiles show a double peak structure and are roughly aligned. In comparing the radio to

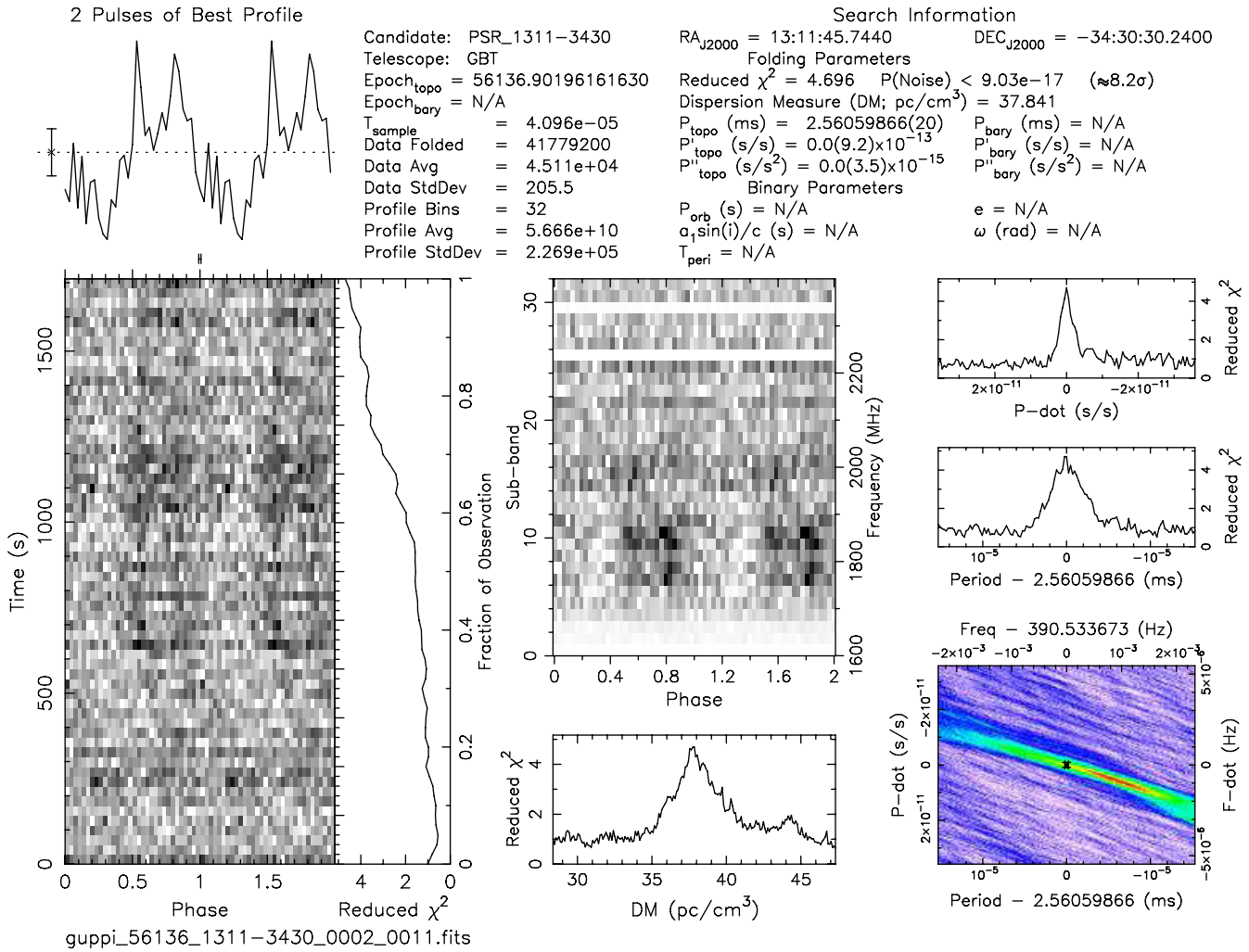

Figure 3. Radio detection of PSR J1311−3430 using the GBT at 2 GHz. This shows a span of 1711 s folded using the ephemeris from Pletsch et al. (2012). The pulsar is very weak during the first 600 s of this interval and appears to show some excess delay as it comes out of eclipse. When the first 600 s are excluded from the analysis, the detection significance is above 10σ. The fact that the detection is strongest in a frequency band of ∼150 MHz and weak in the rest of the band is consistent with interstellar scintillation.

(A color version of this figure is available in the online journal.)

gamma-ray profile alignment, it is important to consider the uncertainty in absolute phasing due to the uncertainty in the DM measurement. The uncertainty in the DM is 0.26 pc cm^{-3}. A change in the DM of this magnitude corresponds to a shift in the relative phasing of the radio and gamma-ray profiles of 0.1 in phase. So, within the uncertainties, either the first radio peak could be aligned with the first gamma-ray peak or the second peaks could be aligned. However, the peak separation in the radio profile is 0.28 ± 0.02 and the gamma-ray peaks are separated by 0.35 ± 0.01, so it not possible for both peaks to be precisely aligned. Finally, the radio profile also may be broadened by scattering but without a higher quality profile or detections at other frequencies; this is hard to quantify.

3. DISCUSSION

This detection demonstrates that although this pulsar would have been extraordinarily difficult to detect in a radio search, it is indeed visible from Earth in the radio band, at least when the conditions in the system permit. The measurement of the pulsar DM yields a distance estimate from the NE2001 galactic free electron density model (Cordes & Lazio 2002) of 1.4 kpc, typical of the LAT-detected MSP sample. Using this distance and the measured proper motion of 8 mas yr^{-1}, we compute that the contribution to the observed period derivative from the Shklovskii effect (Shklovskii 1970) is only 2.7%. Using the DM distance to compute the gamma-ray luminosity gives an efficiency $\eta = L_\gamma/\dot{E} = 30\%$, assuming that the beaming correction f_Ω is 1.

To gauge PSR J1311−3430's significance for the gamma-ray pulsar population, we follow Romani (2012) and restrict our attention to the brightest ∼250 *Fermi* sources, for which extensive counterpart studies (including repeated radio pulse searches) have been made. These include 14 gamma-ray MSPs, all of which have now been detected in radio plus the newly discovered PSR J2339−0533. There are four remaining unassociated objects in this sample—their gamma-ray properties (a significant high-energy spectral cutoff and low spectral variability) mark them as likely pulsars. However, some are at lower Galactic latitudes and so, unlike J1311−3430 and J2339−0533, may be powered by young pulsars. Even if we count all these sources as MSPs undetectable in the radio, the fraction is only $4/18 = 0.22$. This is dramatically lower than the $27/42 = 0.64$ fraction of radio-quiet young pulsars in this sample. We conclude that, for MSPs, radio beams cover nearly as much sky as the gamma-ray beams, and largely overlap. This agrees with

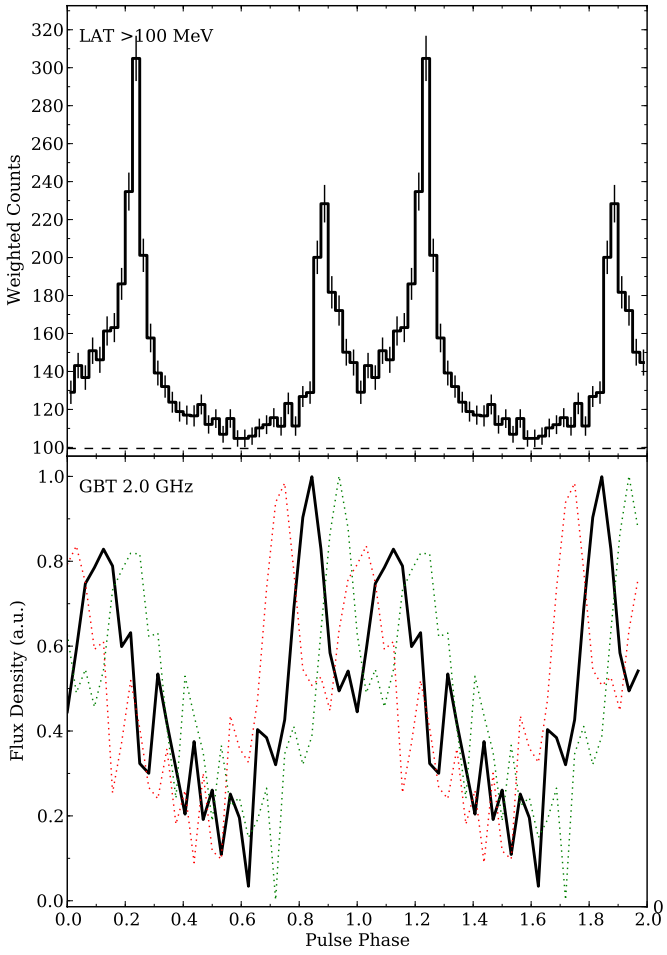

Figure 4. Phase-aligned radio and gamma-ray profiles. The gamma-ray profiles are weighted counts with energies >100 MeV and the radio profile is from the GBT detection of pulsations at 2 GHz. The dotted lines are the same profile phase shifted forward and back by 0.1 in phase, comparable to the DM uncertainty.
(A color version of this figure is available in the online journal.)

previous results showing that the beaming fraction of MSPs is near unity and likely from a fan beam (Lorimer 2008, and references therein). Conversely, the lack of a large number of black-widow-like LAT sources remaining to be detected suggests that there is not a large phase space for binary gamma-ray pulsars that cannot (at least occasionally) be detected in the radio; by the time the wind from the companion is strong enough to completely bury the radio signal, the pulsar accelerator itself may be quenched.

The small fraction of time in which the radio pulsations are detectable is notable. There are several possible explanations that are difficult to differentiate between with only one relatively low signal-to-noise detection. One reason could be simply interstellar scintillation. High-frequency observations of nearby MSPs are particularly susceptible to scintillation. For some of the MSPs found in LAT-directed surveys at Parkes, the observed flux density varies by a factor of 20 from observation to observation and some of the pulsars are detectable in only about one-third of the observations (F. Camilo et al. in preparation). Alternatively, the pulsations could be eclipsed by material local to the system itself. There are several possible mechanisms for such eclipses (see Thompson et al. 1994, for a review) and which mechanism is operative may be different for different systems. In this case, the continuum detections of a radio point source suggest that the pulsations may be scattered out of existence (e.g., scattering by plasma turbulence) rather than the radio waves being actually absorbed. Variations in the scattering medium may be responsible for the non-detections at other times and frequencies. The presence of a red, flaring optical component, likely from the pulsar flux reprocessed in the companion wind (Romani et al. 2012), gives additional evidence for a wind of variable density and covering fraction. The timescale and magnitude of DM variations can be a useful diagnostic of these processes. We see some evidence for DM growing to just over 38.0 pc cm^{-3} in the later part of our observation but the significance is too limited to draw any firm conclusions. Also, it is difficult to constrain the presence of a scattering tail in the pulse profile for the same reasons.

Considering the VLA imaging observations, if a significant portion of the flux at 1.4 GHz is from the point source, it would imply a spectral index of -1.8, typical of known pulsars (Maron et al. 2000), although there is an uncertain contribution from, e.g., a bow shock or pulsar wind nebula. Deeper imaging in a higher resolution array configuration is required to characterize the continuum source and its variability properties.

Within the uncertainties in the absolute phasing, the radio and gamma-ray pulse profiles are approximately aligned, although their peak separations are slightly different, with the radio peaks being closer together than the gamma-ray ones. This could indicate that both are formed in the same geometric region, but at different altitudes.

This detection illustrates that additional observations, particularly at high frequency, are needed to search for radio pulsations from the other strong radio-quiet MSP candidates. Of course, these searches would be much more sensitive with a known pulsation from a gamma-ray detection, as was the case with J1311. Exhaustive searches of the LAT data as well as repeated radio observations are clearly warranted in these cases.

The National Radio Astronomy Observatory is a facility of the National Science Foundation operated under cooperative agreement by Associated Universities, Inc. The Parkes Observatory is part of the Australia Telescope National Facility, which is funded by the Commonwealth of Australia for operation as a National Facility managed by CSIRO. The GMRT is run by the National Centre for Radio Astrophysics of the Tata Institute of Fundamental Research. We thank the staff of the GMRT for help with the observations. The Nançay Radio Observatory is operated by the Paris Observatory, associated with the French Centre National de la Recherche Scientifique (CNRS).

The *Fermi*-LAT Collaboration acknowledges support from a number of agencies and institutes for both development and the operation of the LAT as well as scientific data analysis. These include NASA and DOE in the United States, CEA/Irfu and IN2P3/CNRS in France, ASI and INFN in Italy, MEXT, KEK, and JAXA in Japan, and the K. A. Wallenberg Foundation, the Swedish Research Council, and the National Space Board in Sweden. Additional support from INAF in Italy and CNES in France for science analysis during the operations phase is also gratefully acknowledged.

This work was partially supported by the *Fermi* Guest Observer Program, administered by NASA. The work of C.C.C. was completed while under contract with NRL and supported by NASA DPR S-15633-Y. M.G. acknowledges financial contribution from the agreement ASI-INAF I/009/10/0. We thank John Sarkissian for help with observations at Parkes.

Facilities: GBT (GUPPI), VLA, GMRT, NRT, Parkes

REFERENCES

Ackermann, M., Ajello, M., Allafort, A., et al. 2012, ApJ, 753, 83
Cheung, C. C., Donato, D., Gehrels, N., Sokolovsky, K. V., & Giroletti, M. 2012, ApJ, 756, 33
Condon, J. J. 1997, PASP, 109, 166
Cordes, J. M., & Lazio, T. J. W. 2002, arXiv:astro-ph/0207156
DuPlain, R., Ransom, S., Demorest, P., et al. 2008, Proc. SPIE, 7019, 70191D
Kataoka, J., Yatsu, Y., & Kawai, N. 2012, ApJ, 757, 176
King, A. R., Beer, M. E., Rolfe, D. J., Schenker, K., & Skipp, J. M. 2005, MNRAS, 358, 1501
Kong, A. K. H., Huang, R. H. H., Cheng, K. S., et al. 2012, ApJL, 747, 3
Lorimer, D. R. 2008, LRR, 11, 8
Maron, O., Kijak, J., Kramer, M., & Wielebinski, R. 2000, A&AS, 147, 195
Nolan, P. L., Abdo, A. A., Ackermann, M., et al. 2012, ApJS, 199, 31
Perley, R. A., Chandler, C. J., Butler, B. J., & Wrobel, J. M. 2011, ApJL, 739, 1
Pletsch, H. J., Guillemot, L., Fehrmann, H., et al. 2012, Sci, 338, 1314
Ransom, S. M. 2001, PhD thesis, Harvard Univ.
Ransom, S. M., Ray, P. S., Camilo, F., et al. 2011, ApJL, 727, 16
Ray, P. S. 2012, Talk Given at the Fourth International Fermi Symposium
Ray, P. S., Abdo, A. A., Parent, D., et al. 2012, in Proc. 2011 Fermi Symposium, ed. A. Morselli, eConf 110509
Ray, P. S., Kerr, M., Parent, D., et al. 2011, ApJS, 194, 17
Romani, R. W. 2012, ApJL, 754, 25
Romani, R. W., Filippenko, A. V., Silverman, J. M., et al. 2012, ApJ, 760, 36
Romani, R. W., & Shaw, M. S. 2011, ApJL, 743, 26
Roy, J., Gupta, Y., Pen, U.-L., et al. 2010, ExA, 28, 55
Shklovskii, I. S. 1970, SvA, 13, 562
Thompson, C., Blandford, R. D., Evans, C. R., & Phinney, E. S. 1994, ApJ, 422, 304